Carbonylation Caused by Cigarette Smoke Extract Is Associated with Defective Macrophage Immunity

Steven Bozinovski[1], Ross Vlahos[1], Yilin Zhang[1], Lin Chin Lah[1], Huei Jiunn Seow[1], Ashley Mansell[3], and Gary P. Anderson[1,2]

[1]Department of Pharmacology, and [2]Department of Medicine, University of Melbourne, Melbourne, Victoria, Australia; and [3]Centre for Innate Immunity and Infectious Disease, Monash Institute of Medical Research, Clayton, Victoria, Australia

Oxidants in cigarette smoke inhibit pathogen recognition receptor function and phagocytosis, but the molecular basis of this inhibition remains obscure. We sought to identify the inhibitory mechanisms that impair alveolar macrophage function. Balb/c mice were acutely exposed to four cigarettes for 4 hours before treatment with intranasal LPS (1 μg). The mice exhibited significantly reduced airway neutrophilia and expression of TNF-α. Balb/c-derived MH-S alveolar macrophage cells exposed to cigarette smoke extract (CSE) displayed a similar inhibitory response to stimulation with LPS. The induction of inflammatory genes by recombinant (r) TNF-α (100 ng/ml) was also impaired by CSE. Because both pathways converge on NF-κB, the degradation of IκBα and the phosphorylation of p65 were assessed and shown to be blunted by CSE. CSE also blocked the activity of activator protein-1 (AP-1) by inhibiting p38 mitogen activated protein kinase (MAPK) in a reduced glutathione (GSH)-reversible manner. The induction of specific Toll-like receptor (TLR)–negative regulators (suppressor of cytokine signaling-1 [SOCS-1], interleukin-1 receptor associated kinase-M [IRAK-M], and IL-10) did not account for the impaired responses of TLRs. As free radical species are abundant in CSE and GSH restored function, a panel of oxidative/nitrosative stress markers was screened using immunocytochemistry. The panel identified protein carbonylation as the major CSE-inducible marker. Oxyblot analysis confirmed that CSE potently introduced carbonyl groups to many proteins in a dose-dependent and time-dependent manner that inversely correlated with the expression of TNF-α. The formation of pseudopodia was not prevented, but these membrane extensions were heavily carbonylated, and primary alveolar macrophages were also targeted for carbonylation. Oxidants in cigarette smoke drive a rapid, persistent, and global protein carbonylation that may represent a common pathway to altered immunity in disease.

Keywords: carbonylation; macrophage immunity; TLR signaling

Cigarette smoking and exposure to environmental tobacco smoke (ETS) are significant risk factors for respiratory infection (1). Approximately 30% of hospital admissions for pneumonia in children were estimated to be attributable to ETS (2). Because pneumonia is already the leading cause of mortality and morbidity in children worldwide, the impact of ETS on respiratory illnesses is likely to increase as smoking rates rise in developing regions, including Asia and Africa (3). The molecular nature of increased susceptibility to microbial infection is not fully understood. Smoking and ETS exert diverse effects on the immune system by altering important host defense mechanisms (4). Repeated exposure to irritants in smoke directly damages the respiratory epithelium, leading to increased permeability and impaired mucociliary clearance (5). We previously showed that cigarette smoke extract (CSE) also attenuates the release of inflammatory mediators by lung epithelial cells in response to the microbial ligand LPS (6). A similar decline in mediator release is evident in lung macrophages and monocytes, and is associated with a reduced activation of the proinflammatory transcription factor NF-κB (7–10).

The host normally responds to infection by recognizing a suite of pathogen-associated molecular patterns (PAMPs) via specialized pathogen recognition receptors (PRRs) such as Toll-like receptors (TLRs), which promote the release of multiple inflammatory mediators. A loss of PRR function will therefore adversely affect essential innate immune responses. Exposure to smoke also impairs the macrophage-mediated efferocytosis of apoptotic cells (11) and the phagocytosis of bacteria (12, 13). However, the mechanisms that drive this impaired recognition and clearance remain elusive. A number of reports implicate free radicals as the major immunosuppressive mediator in cigarette smoke, because scavengers including reduced glutathione (GSH) and *N*-acetylcysteine (NAC) restore the normal release of inflammatory mediators (6, 7, 14, 15). This is consistent with the very high oxidant/free radical burden in cigarette smoke, which includes superoxide ($O_2\cdot$), hydroxyl radicals ($\cdot OH$), hydrogen peroxide (H_2O_2), nitric oxide (NO), and peroxynitrite species (16).

Because the relative roles of oxidative and nitrosative markers in smoke-mediated macrophage dysfunction have not been comprehensively evaluated, a panel of stress markers was screened via immunocytochemistry (ICC), Western blot analysis, and selective biochemical assays. Of the five alternative oxidative/nitrosative stress markers screened, only protein carbonylation was rapidly induced by CSE in a manner reversed by treatment with exogenous GSH. The detection of protein carbonylation is the most widely used marker for protein oxidation by the derivatization of modified carbonyl groups (aldehydes and ketones) at cysteine, arginine, histidine, lysine, proline, or threonine residues (17, 18), and is a major pathway to protein oxidation (19). Furthermore, the degree and duration of CSE-mediated protein carbonylation were correlated with the expression of the inflammatory mediator, TNF-α. Our novel findings demonstrate that protein carbonylation by CSE occurs in a rapid and global manner, and as a result, essential macrophage functions, including pathogen sensing and the internalization and release of inflammatory mediators, are all significantly compromised.

MATERIALS AND METHODS

Reagents

Anti-4HNE rabbit polyclonal antibody was purchased from Alpha Diagnostics (San Antonio, TX). Anti-glutathione monoclonal antibody was purchased from Virogen (Watertown, MA). Anti-p65, phospho-p65, IκBα, phospho-p38, pErk1/2, pJNK, and nitro-tyrosine rabbit polyclonal antibodies were purchased from Cell Signaling Technologies (Danvers, MA). Commercial ELISA sets were purchased from R&D Systems (Minneapolis, MN). Recombinant TNF-α (rTNF) was

(*Received in original form June 29, 2010 and in final form August 19, 2010*)

This work was supported by the National Health and Medical Research Council of Australia.

Correspondence and requests for reprints should be addressed to Steven Bozinovski, Ph.D., Department of Pharmacology, University of Melbourne, Melbourne 3010, Victoria, Australia. E-mail: bozis@unimelb.edu.au

This article has an online supplement, which is accessible from this issue's table of contents at www.atsjournals.org

Am J Respir Cell Mol Biol Vol 45. pp 229–236, 2011
Originally Published in Press as DOI: 10.1165/rcmb.2010-0272OC on October 8, 2010
Internet address: www.atsjournals.org

purchased from Prospec (Ness-Ziona, Israel). All other reagents were purchased from Sigma (St. Louis, MO).

Exposure to Cigarette Smoke

Balb/c mice were exposed to cigarette smoke as previously described (20), with minor modifications. Mice were exposed to smoke generated from one cigarette (2R4F; University of Kentucky, Lexington, KY) for 15 minutes. This process was repeated three times for a total of four cigarettes over a 4-hour period. Two hours after the final cigarette, mice were treated intranasally with saline or LPS (1 μg) and bronchoalveolar lavage fluid (BALF)/excised lungs were archived, as previously described (21). For the myeloperoxidase (MPO) analysis of lung tissue, refer to the online supplement.

Preparation of CSE

CSE was prepared as previously described, with minor modifications (6). Briefly, one research filtered cigarette (2R4F; University of Kentucky) was bubbled through 25 ml of RPMI medium. This preparation was filtered through a 0.2-μm filter, and was arbitrarily assigned the value "1" (one cigarette in 25 ml). For GSH experiments, CSE was incubated with 0.1 mM GSH for 10 minutes at room temperature before the treatment of cells.

Cell Culture

Murine MH-S alveolar macrophages (CRL-2019; American Type Culture Collection, Manassas, VA) are a noncancer immortalized cell line that retains many morphologic and functional properties of primary alveolar macrophages (22). MH-S cells also effectively adhere to and clear bacteria by phagocytosis and phagolysosomal processing (13). MH-S cells were exposed to CSE for a short 15-minute pulse. After treatment with CSE, cells were maintained in RPMI-1640 + 1% FCS for the indicated recovery period, before challenge with 1 μg/ml LPS or 100 ng/ml rTNF-α.

Phagocytosis and Molecular Assays

The phagocytic function of MH-S cells was quantified using the Vybrant Phagocytosis Kit (Invitrogen, Carlsbad, CA), according to the manufacturer's instructions. The intracellular uptake of fluorescein-labeled *Escherichia coli* was preferentially detected by extracellular quenching with Trypan blue. Real-time quantitative (Q) PCR was performed using Taqman chemistry, as previously described (23). For the assessment of NF-κB and activator protein-1 (AP-1) DNA binding activity, nuclear extraction and electromobility shift assay (EMSA) were performed as previously described (6). Western blot analysis was also performed as previously described (24). For the detection of S-nitrosylated proteins, a modified biotin switch method was performed, according to the manufacturer's instructions (Cayman Chemicals, Ann Arbor, MI).

Methanol-fixed MH-S cells grown in 8-well chambers were fixed in ice-cold methanol for 10 minutes, and staining was performed using a DAKO Envision Staining Kit (DAKO, Inc. La Jolla, California, Carpentaria, CA).

Detection of Carbonylation

The detection of protein carbonylation was performed using a Protein Oxidation Detection Kit (Millipore, Billerica, MA), according to the manufacturer's instructions. For the detection of protein carbonylation by immunocytochemistry (ICC), cells were incubated with 1 × 2,4-dinitrophelylhydrazine after the fixation step, and staining proceeded as already described.

Statistical Analysis

Differences between groups were analyzed using an unpaired *t* test or two-way ANOVA, followed by a Bonferroni multiple comparison test (GraphPad Software, Inc. La Jolla, CA). $P < 0.05$ was considered significant.

RESULTS

CSE-Mediated Suppression of Phagocytosis and Inflammatory Gene Expression Is Independent of LPS Tolerance Mechanisms

A smoke exposure model of four cigarettes over a 4-hour period was sufficient to reduce LPS-mediated BAL neutrophilia (Figure 1A) and tissue leukocyte accumulation, as detected by the activity of MPO (Figure 1B) in BALB/c mice. This reduction in neutrophil recruitment was similar to the significant reduction in TNF-α lung mRNA (Figure 1C) and secreted protein in BALF (Figure 1D). To investigate the molecular mechanisms behind impaired innate immunity, MH-S alveolar macrophages that retained the functional properties of primary alveolar macrophages (13, 22) were used. A CSE dose response was first performed, demonstrating the dose-dependent inhibition of TNF-α (Figure 2A). One CSE (1 cigarette in 25 ml of medium) was subsequently used, because this dose displayed inhibitory activity similar to that of the *in vivo* whole-smoke model without affecting cell viability. Similar doses were also used with no detrimental effects on cell viability (13, 25), although direct comparisons are complicated because of the alternative methods used to generate stock CSE solutions. Because the recognition and ingestion of pathogen are integral to a host's innate defense system, we quantitatively measured the phagocytosis of fluorescently labeled *E. coli* in MH-S alveolar macrophages. As shown in Figure 2B, the internalization of FITC–*E. coli* over the 2-hour incubation period was reduced by CSE. A more detailed kinetic analysis of TNF-α mRNA (Figure 2C) and secreted protein (Figure 2D) demonstrated the sustained nature of CSE-mediated macrophage suppression.

A secondary event during acute inflammatory responses to pathogens and other foreign agents is the resolution of inflammation. The engagement of TLRs promotes negative feedback mechanisms, including the release of inhibitory mediators to limit sustained activation (26). Because CSE contains detectable concentrations of LPS (27, 28), negative TLR regulators (suppressor of cytokine signaling-1 [SOCS-1], IL-10, and interleukin-1 receptor associated kinase-M [IRAK-M]) were measured by QPCR, and were not induced by CSE (Table 1). The oxidative stress response marker, heme oxygenase–1 (HO-1), was elevated by CSE treatment (6-fold), and no increase in apoptosis was detected as determined by acridine orange/ethidium bromide staining and fluorescence microscopy (Table 1).

Free Radical Species Inhibit Multiple Signaling Intermediates That Control NF-κB and AP-1 Activity

To investigate the importance of reactive radical species, CSE was pretreated with GSH, which dose-dependently restored the LPS-induced expression of TNF-α, as assessed by QPCR (Figure 3A). The restoration of TNF-α protein was maximally achieved when CSE was pretreated with GSH (Figure 3B). Simultaneous treatment with CSE and GSH was less effective, and the delivery of GSH after CSE was completely ineffective in restoring LPS responses. In addition to TNF-α, the CSE-mediated suppression of the alternative TLR-4 marker, as induced by interferon regulatory factor (IRF) signaling (interferon gamma–induced protein-10 [IP-10], Figure 3C) and by IL-6 (Figure 3D), was

TABLE 1. EXPRESSION OF NEGATIVE REGULATORS AND VIABILITY IN RESPONSE TO CIGARETTE SMOKE EXTRACT

	Fold Increase (VEH)				
$n = 3$	HO-1	IL-10	SOCS1	IRAK	Viability (% VEH)
CSE (3 hr) mean (SE)	6.5 * (1.1)	1.6 (0.8)	0.6 (0.4)	0.8 (0.1)	91 (14)

Definition of abbreviations: CSE, cigarette-smoke extract; HO, heme oxygenase-1; SE, standard error; SOC-1, suppressor of cytokine signaling-1; IRAK, IL-1 receptor associated kinase; VEH, vehicle.

*$P < 0.05$.

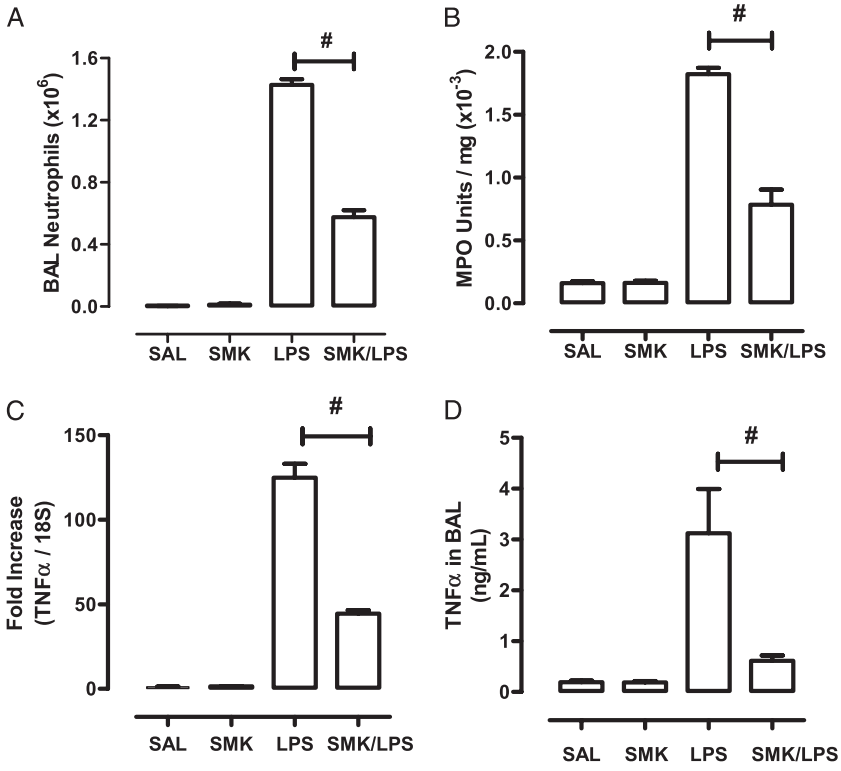

Figure 1. Acute exposure to smoke impaired LPS-induced neutrophil recruitment and induction of TNF-α. BALB/c mice were exposed to cigarette smoke (SMK) over a 4-hour period before intranasal delivery of saline (SAL) or 1 μg LPS. (*A*) Bronchoalveolar lavage (BAL) neutrophil numbers and (*B*) Myeloperoxidase (MPO) activity in lung tissue were measured 24 hours after the challenge. Lungs were also collected 2 hours after treatment with LPS, and (*C*) TNF-α mRNA levels and (*D*) secreted protein concentrations in BAL were determined. Data are expressed as mean ± SEM (n = 6–8, $^{\#}P < 0.05$).

restored by GSH. When cells were stimulated with rTNF-α instead of LPS, a similar decline in the expression of TNF-α and IL-6 was evident (Figures 3E and 3F). The maximal activation of NF-κB requires the degradation of the inhibitor of κBα (IκBα) and the phosphorylation of p65. Treatment with CSE markedly delayed the degradation of IκBα and suppressed the phosphorylation of p65, which correlated with reduced NF-κB DNA binding in a GSH-reversible manner (Figure 4A). The engagement of TLR-4 also promotes the phosphorylation of mitogen-activated protein kinases (MAPK), which can differentially regulate the AP-1 heterodimeric transcription factor complex consisting of fos and jun subunits. We found that all three MAPKs, including c-Jun N-terminal kinase (JNK), p38, and extracellular-signal regulated kinase 1/2 (Erk1/2) were phosphorylated in response to LPS in alveolar macrophages. In addition, JNK was directly activated by exposure to CSE. However, only the activation of p38 was blocked by CSE in a GSH-responsive manner (Figure 4B), implicating p38 as the main MAPK susceptible to CSE (Figure 4B, *bottom*).

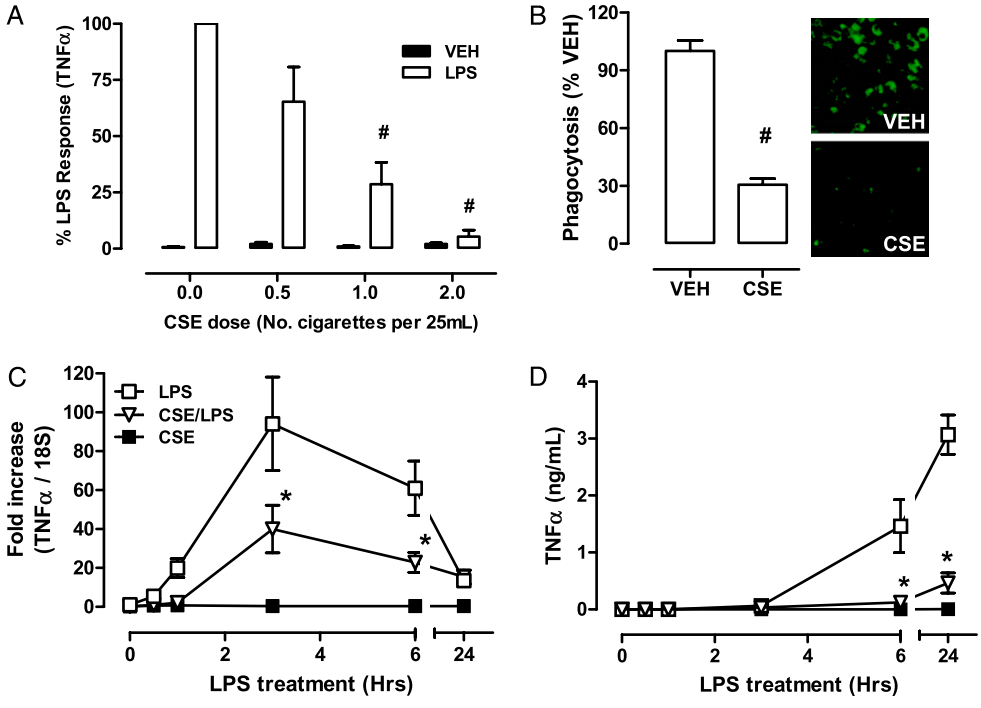

Figure 2. Phagocytosis and inflammatory gene expression are suppressed by 15-minute pretreatment with cigarette smoke extract (CSE). (*A*) MH-S cells were exposed to indicated doses of CSE before challenge with LPS (1 μg/ml) for 24 hours, and secreted TNF-α concentrations in supernatants were measured by ELISA. (*B*) MH-S cells were treated with CSE or vehicle (VEH) for 15 minutes, allowed to recover for 1 hour, and then challenged with FITC–*Escherichia coli*. Images were captured by fluorescent microscopy, and the intensity of fluorescence was quantified using a FlexStation II microplate reader (Silicon Valley, CA) and presented as a percentage of VEH-treated cells. (*C* and *D*) MH-S cells were treated with CSE or VEH for 15 minutes and then challenged with LPS for 24 hours. At indicated time points, TNF-α mRNA (*C*) and secreted protein (*D*) concentrations were measured by quantitative (Q) PCR and ELISA. Data are expressed as mean ± SEM (n = 3–5, $^{\#}P < 0.05$).

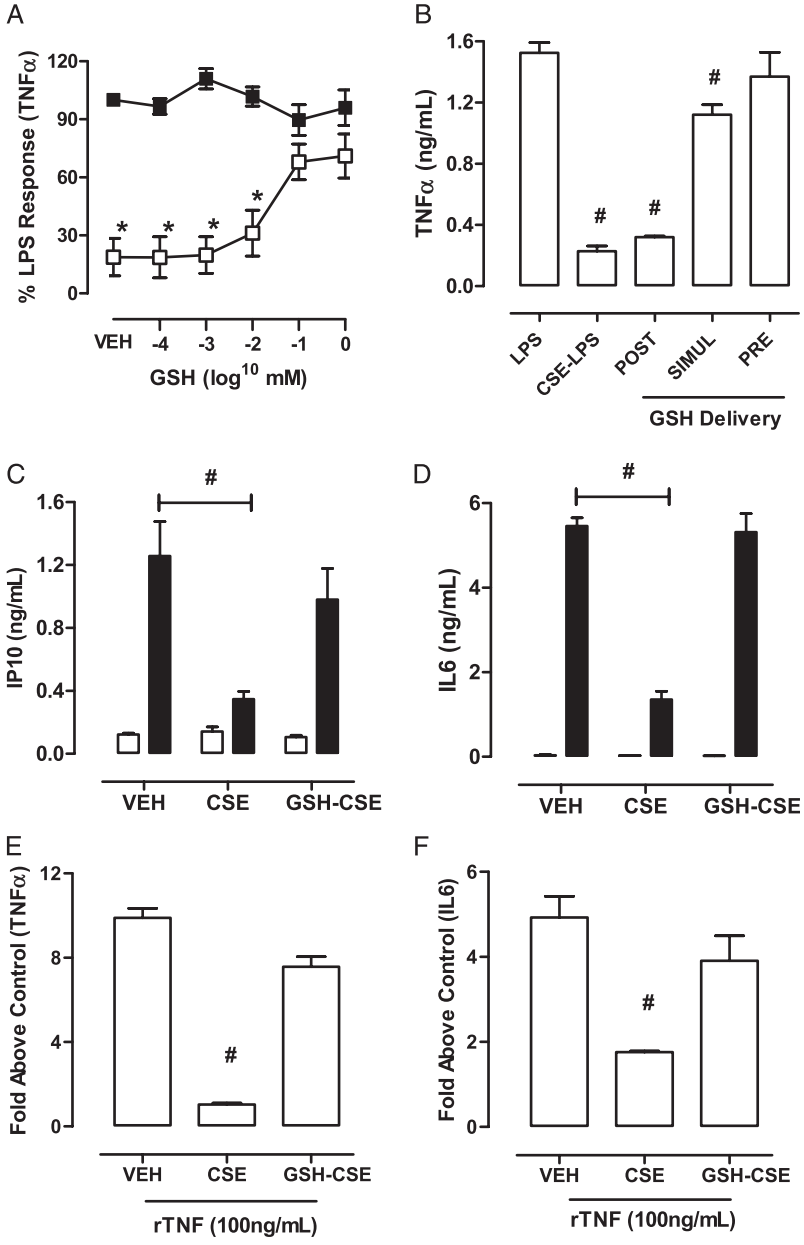

Figure 3. Pretreatment with glutathione (GSH) maximally restores inflammatory responses, and CSE also impairs recombinant (r) TNF-α activity. (*A*) MH-S cells were treated with CSE (*open squares*), preincubated with increasing concentrations of GSH or VEH (*solid squares*), allowed to recover for 1 hour in fresh media, and then challenged with LPS for 3 hours before assessing TNF-α levels by QPCR. (*B*) CSE was pretreated with GSH (PRE), simultaneously added to cells with CSE (SIMUL), or added to cells after exposure to CSE (POST), followed by challenge with LPS and measurement of TNF-α by ELISA. (*C* and *D*) Cells were exposed to CSE alone or CSE pretreated with GSH for 15 minutes, followed by a 1-hour recovery period, and were then stimulated with LPS for 24 hours. Concentrations of secreted interferon gamma induced protein-10 (IP-10) (*C*) and IL-6 (*D*) in supernatants were determined by ELISA. (*E* and *F*) After treatment with CSE, cells were treated with rTNF-α (100 ng/ml) for 3 hours, and TNF-α/IL-6 levels were determined by QPCR. Data are expressed as mean ± SEM ($n = 3$–5, $^{\#}P < 0.05$).

Rapid and Sustained Induction of Protein Carbonylation Is Associated with Impaired Expression of TNF-α and Phagocytosis

Because CSE-derived free radical species drive suppressed inflammation, a panel of oxidative and nitrosative stress markers was screened by ICC, including protein carbonylation, S-nitrosylation, 4HNE, S-glutathionylation, and nitro-tyrosine. As shown in Figure 5A, only protein carbonylation was markedly enhanced by exposure to CSE. No further increase in S-nitrosylation was evident according to ICC, and this result was also validated by the biotin switch method (Figure 5B). Global S-glutathionylation or 4HNE were not altered by exposure to CSE (Figure E1), and nitro-tyrosine staining was not evident above the isotype control background (data not shown). Oxyblot analysis confirmed CSE as a potent inducer of carbonylation that targets many proteins within the 40–100-kD range in a dose-dependent manner (Figure 6A), which was inversely correlated with the LPS-induced expression of TNF-α (Figure 2A). Subcellular analysis revealed extensive carbonylation in the cytosolic, nuclear, and membrane fractions (Figure E2). Protein carbonylation also occurred very rapidly within 10 minutes of exposure to CSE, and the modification persisted for at least 6 hours, slowly resolving by 24 hours (Figure 6B, *inset*). The kinetics of CSE-mediated carbonylation was again inversely correlated with the production of TNF-α, because a maximal restoration of gene expression was evident at the 24-hour time point (Figure 6B). Preincubating CSE with GSH and *N*-acetylcysteine (NAC) prevented the carbonylation of MH-S cells, whereas ascorbate proved ineffective (Figure 6C). The pattern of carbonylation was again inversely associated with the LPS-induced expression of TNF-α, where GSH and NAC restored normal responses, in contrast to ascorbate (Figure 6D).

Heavily Carbonylated Pseudopod Extensions Fail to Internalize Bacteria

We used differential interference contrast light microscopy to investigate the morphology of macrophages in the presence of CSE, and to localize further intracellular regions positive for protein carbonylation. As shown in Figure 6E (*top*), the for-

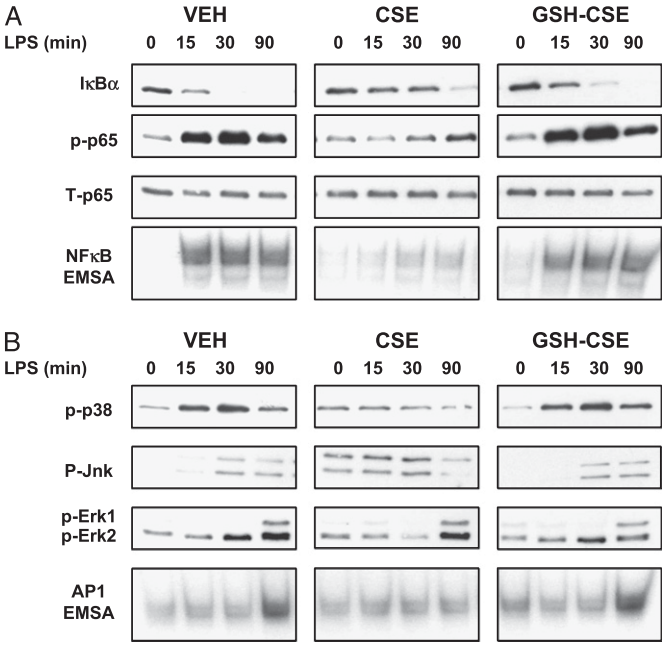

Figure 4. CSE impairs signaling to NF-κB and activating protein–1 (AP-1) in a GSH-sensitive manner. MH-S cells were pretreated with VEH, CSE, or CSE prepared with GSH (GSH-CSE) for 15 minutes, followed by 1 hour of recovery in fresh medium, and were then stimulated with LPS over indicated time points. (*A*) Western blot analysis was used to measure IκBα, the phosphorylated p65 subunit of NF-κB (p-p65), and total p65 (T-p65). The DNA binding activity of NF-κB was also determined by electromobility shift assay (EMSA). (*B*) The activity of mitogen-activated protein kinase (MAPK) was determined by Western blot analysis, using phospho-specific antibodies to p38, c-Jun N-terminal kinase (JNK), and extracellular signal–regulated kinase 1/2 (Erk1/2). AP-1 activity was assessed by EMSA, as described in MATERIALS AND METHODS. Images are representative of three individual experiments.

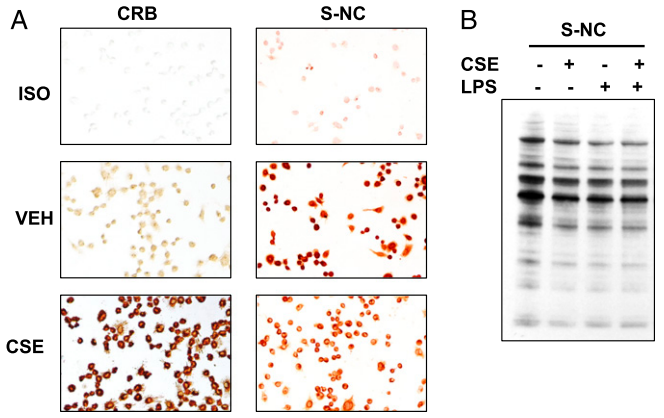

Figure 5. CSE selectively promotes the induction of protein carbonylation. MH-S cells cultured in 8-well chamber slides were pretreated with VEH or CSE for 15 minutes, followed by 1 hour of recovery in fresh medium, and were then subjected to immunocytochemistry (ICC) for stress markers, including protein carbonylation (CRB) and S-nitrosylation (S-NC). An isotype control (ISO) was also performed on CSE-treated cells. Images are representative of three individual experiments. (*B*) S-nitrosylation levels were also determined, using the biotin switch method (as detailed in MATERIALS AND METHODS).

mation and extension of pseudopodia were evident in CSE-treated cells that were abundantly carbonylated by CSE in a GSH-sensitive manner (Figure 6E, *top*). Because phagocytic receptors cluster in outer membrane regions, we assessed whether localized carbonylation was associated with impaired phagocytosis. The CSE-mediated suppression of bacterial ingestion was completely restored by GSH (Figures 6E, *bottom*, and 6F).

Primary Alveolar Macrophages Are Also Targeted for Protein Carbonylation

Carbonylation levels were assessed in primary alveolar macrophages isolated from Balb/c mice by BAL. As shown via ICC in Figure 7A, CSE induced global carbonylation. These findings were also validated by oxyblot analysis, demonstrating a marked induction of protein carbonylation by CSE, whereas LPS alone caused no change (Figure 7B). Consistent with MH-S cells, pretreatment with CSE for 15 minutes inhibited the LPS-induced expression of TNF-α in primary alveolar macrophages (Figure 7C).

DISCUSSION

The biological consequences of free radical exposure are diverse, and include direct modifications and damage of DNA, lipids, and many proteins. Alveolar macrophage phagocytosis is impaired in chronic lung disorders such as chronic obstructive pulmonary disease (29), where exposure to smoke causes significant oxidative damage. Cigarette smoke also impairs the clearance of apoptotic cells through the oxidant-dependent activation of Ras homolog gene family, member A (RhoA) (30) and the inhibition of Ras-related C3 botulinum toxin substrate 1 (Rac1) (31), leading to defective actin polymerization, normally required for efficient efferocytosis. Here, we observed that macrophage pseudopodia were heavily carbonylated in response to cigarette smoke exposure. Because carbonylation was previously identified as a major mechanism in actin cytoskeletal instability (32–34), our findings strongly implicate cigarette smoke-mediated carbonylation in defective efferocytosis and pathogen clearance. The defect appears to be selective, because the phagocytosis of polystyrene latex beads by PRR-independent mechanisms was unaltered in smokers (35).

We found that LPS-induced NF-κB translocation and transactivation pathways were also compromised by CSE in an oxidant-dependent manner. The induction of inflammatory genes by rTNF-α was similarly reduced. Because the engagement of TNF receptor and TLR-4 converge at IκB kinase (IKK) to activate NF-κB, oxidants in CSE are likely targeting IKK or its downstream adaptors. In addition, the observed defect in phagocytosis, AP-1 DNA binding, and IRF-mediated gene expression highlight the diversity of the CSE-mediated inhibition of inflammatory pathways, and favor a model where multiple host defense regulatory proteins are modified by CSE-derived oxidants. Transcription factors such as NF-κB are particularly redox-sensitive, and are therefore very susceptible to oxidative damage. Thus, the degree and constitution of oxidants have the potential to either increase or reduce inflammatory responses, and may even coexist in disease. The findings of this study suggest that smoke mediates impaired primary responses by suppressing bacterial phagocytosis and activation of the TLR-4 pathway, consequent to extensive protein carbonylation.

Exposure to cigarette smoke also markedly depletes intracellular stores of GSH, leading to the generation of oxidized glutathione (GSSG) (7, 36), and the disruption of GSH metabolism is considered a key susceptibility feature of lung diseases (37). Although no global changes in S-nitrosylation, S-glutathionylation,

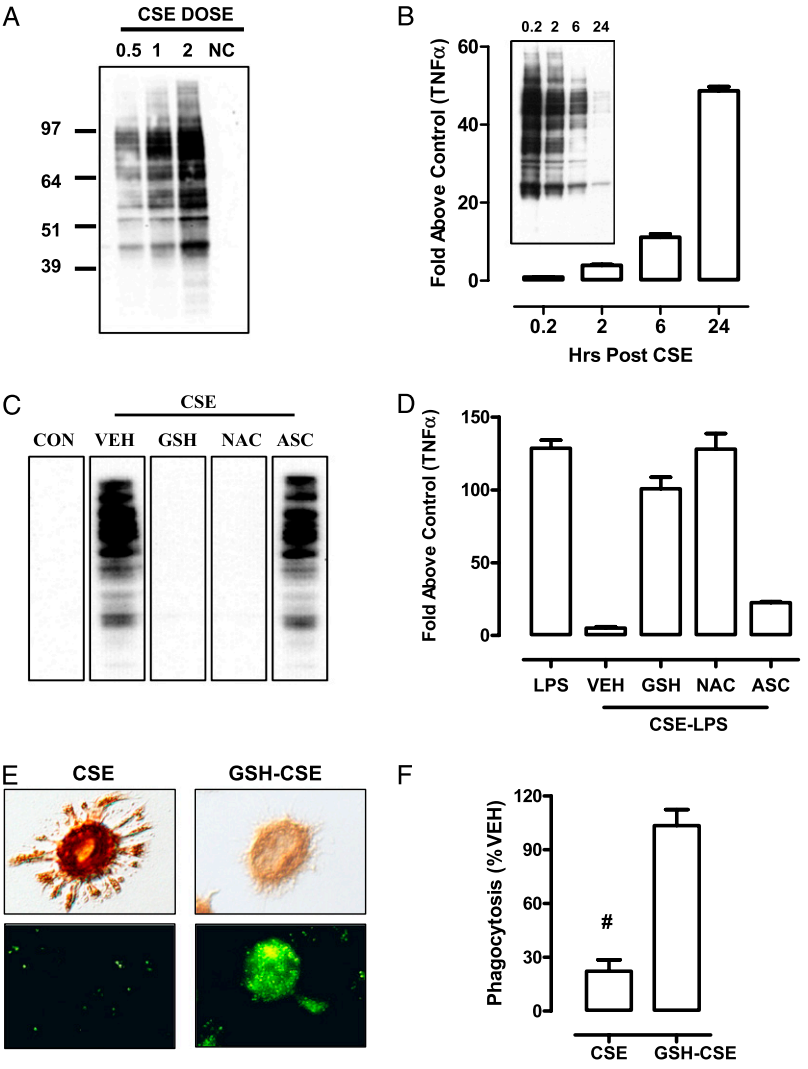

Figure 6. CSE-mediated carbonylation is associated with a loss of TNF-α expression and phagocytosis. (*A*) Oxyblot analyses of MH-S cells, treated with CSE at indicated doses. (*B*) Blot (*inset*) represents carbonylation levels at indicated recovery time points after treatment with CSE, and graph shows levels of TNF-α (QPCR) after 2 hours of treatment with LPS. (*C*) Oxyblot analysis was performed on cells treated with CSE and preincubated with VEH, 0.1 mM GSH, *N*-acetylcysteine (NAC), or ascorbate (ASC). (*D*) After treatment with CSE preincubated with selective antioxidants, cells were stimulated with LPS for 3 hours, and the expression of TNF-α was assessed by QPCR. (*E*) Cells cultured in 8-well chamber slides were fixed and subjected to ICC for protein carbonylation (*E*, *top*), and images were captured using differential interference contrast microscopy. For the assessment of phagocytosis, cells were treated with FITC–*E. coli* after CSE. Images were captured using fluorescent microscopy (*E*, *bottom*). (*F*) The intensity was quantified using a FlexStation II microplate reader, where values are presented as a percentage of VEH-treated cells. Images are representative of three separate experiments. Data are expressed as mean ± SEM ($n = 3$, $^{\#}P < 0.05$).

or 4HNE adduct formation were evident in this study, individual protein modifications may also contribute to altered macrophage function in the presence of cigarette smoke radicals. For example, the generation of intracellular oxidized GSSG pools can drive S-glutathionylation (38), which suppresses the NF-κB pathway by targeting key protein cysteine residues (39). Reactive nitrogen radicals can also directly inhibit NF-κB signaling via the S-nitrosylation of p50 and IKK2 (40). Endogenous NO production via the induction of NO synthases may even provide a physiologic brake via S-nitrosylation, which promotes the resolution of inflammation (41). The observed staining pattern for S-nitrosylation may also reflect the production of constitutive nitric oxide by alveolar macrophages that maintain cellular quiescence during periods of inactivation. Peroxynitrite, a highly reactive product formed in the presence of NO and $O_2^{\cdot}$, can also promote the nitration of susceptible tyrosine residues, including the p65 subunit of NF-κB, leading to a rapid inhibition of DNA binding and gene expression (42).

In this study, protein oxidation by direct carbonylation was highly induced by CSE, and was fully reversed by treatment

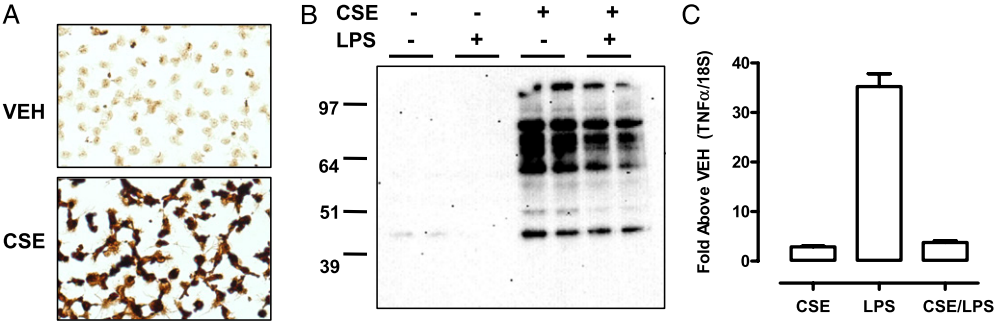

Figure 7. CSE-mediated carbonylation impairment of TNF-α expression occurs in primary alveolar macrophages. (*A*) Primary alveolar macrophages isolated from Balb/c mice by BAL were cultured in 8-well chamber slides and treated with VEH or CSE for 15 minutes, followed by 1 hour of recovery. Fixed cells were then subjected to ICC for carbonylation (CRB). (*B*) Oxyblot analysis was performed on primary alveolar macrophages treated with CSE for 15 minutes, and after 1 hour of recovery, were stimulated with LPS for 2 hours. (*C*) TNF-α levels, as measured by QPCR, were determined after treatments as already described, and expressed as fold increase above VEH.

with GSH and NAC. CSE-mediated protein carbonylation was described to occur via an intracellular metal–catalyzed pathway, because the cell-permeable metal chelator prevented protein oxidation (43). Proteosomal degradation was also identified as a primary mechanism for the removal of carbonylated proteins (44). Hence, the significant delay in macrophage inflammatory responses is consistent with the removal of carbonylated proteins by proteosomal degradation and the gradual synthesis of new protein pools that are functionally active.

According to estimates, approximately 10% of the entire proteome can be carbonylated during aging, starvation, or disease (45). Carbonylated proteins in the lungs of children with pneumonia and other chronic pulmonary diseases have been detected, including α-1 antitrypsin and surfactant protein A (SP-A) (46). Importantly, increased susceptibility to experimental pneumonia and impaired phagocytosis were recently associated with increased SP-A carbonylation, as mediated by exposure to ozone (47). Our study suggests that many PRRs and other associated signaling intermediates are also likely to be modified, underscoring the rationale of targeting oxidative stress but also pointing out major therapeutic hurdles. The degree of carbonylation observed was so rapid and extensive that therapies directed at single moieties seem unlikely to be able to restore function. More importantly, GSH was most effective when allowed time to scavenge reactive intermediates, because the therapeutic delivery of extracellular GSH after exposure to smoke failed to control protein oxidation. Collectively, these data point to a potentially important role of carbonylation in the regulation of host defense. By inference, a reduction in carbonylation may represent a more useful biomarker for antioxidant therapies than current markers, and strategies to limit carbonylation may be useful in preserving and restoring defective mucosal immunity.

Author Disclosure: None of the authors has a financial relationship with a commercial entity that has an interest in the subject of this manuscript.

References

1. Arcavi L, Benowitz NL. Cigarette smoking and infection. *Arch Intern Med* 2004;164:2206–2216.
2. Suzuki M, Thiem VD, Yanai H, Matsubayashi T, Yoshida LM, Tho LH, Minh TT, Anh DD, Kilgore PE, Ariyoshi K. Association of environmental tobacco smoking exposure with an increased risk of hospital admissions for pneumonia in children under 5 years of age in vietnam. *Thorax* 2009;64:484–489.
3. Liu BQ, Peto R, Chen ZM, Boreham J, Wu YP, Li JY, Campbell TC, Chen JS. Emerging tobacco hazards in China: 1. Retrospective proportional mortality study of one million deaths. *BMJ* 1998;317: 1411–1422.
4. Stampfli MR, Anderson GP. How cigarette smoke skews immune responses to promote infection, lung disease and cancer. *Nat Rev Immunol* 2009;9:377–384.
5. Dye JA, Adler KB. Effects of cigarette smoke on epithelial cells of the respiratory tract. *Thorax* 1994;49:825–834.
6. Laan M, Bozinovski S, Anderson GP. Cigarette smoke inhibits lipopolysaccharide-induced production of inflammatory cytokines by suppressing the activation of activator protein–1 in bronchial epithelial cells. *J Immunol* 2004;173:4164–4170.
7. Birrell MA, Wong S, Catley MC, Belvisi MG. Impact of tobacco-smoke on key signaling pathways in the innate immune response in lung macrophages. *J Cell Physiol* 2008;214:27–37.
8. Chen H, Cowan MJ, Hasday JD, Vogel SN, Medvedev AE. Tobacco smoking inhibits expression of proinflammatory cytokines and activation of IL-1R-associated kinase, p38, and NF-kappaB in alveolar macrophages stimulated with TLR2 and TLR4 agonists. *J Immunol* 2007;179:6097–6106.
9. Gaschler GJ, Zavitz CC, Bauer CM, Skrtic M, Lindahl M, Robbins CS, Chen B, Stampfli MR. Cigarette smoke exposure attenuates cytokine production by mouse alveolar macrophages. *Am J Respir Cell Mol Biol* 2008;38:218–226.
10. Vayssier M, Favatier F, Pinot F, Bachelet M, Polla BS. Tobacco smoke induces coordinate activation of HSF and inhibition of NFkappaB in human monocytes: effects on TNFalpha release. *Biochem Biophys Res Commun* 1998;252:249–256.
11. Hodge S, Hodge G, Ahern J, Jersmann H, Holmes M, Reynolds PN. Smoking alters alveolar macrophage recognition and phagocytic ability: implications in chronic obstructive pulmonary disease. *Am J Respir Cell Mol Biol* 2007;37:748–755.
12. King TE Jr, Savici D, Campbell PA. Phagocytosis and killing of *Listeria* monocytogenes by alveolar macrophages: smokers versus nonsmokers. *J Infect Dis* 1988;158:1309–1316.
13. Marti-Lliteras P, Regueiro V, Morey P, Hood DW, Saus C, Sauleda J, Agusti AG, Bengoechea JA, Garmendia J. Nontypeable *Haemophilus influenzae* clearance by alveolar macrophages is impaired by exposure to cigarette smoke. *Infect Immun* 2009;77:4232–4242.
14. McMaster SK, Paul-Clark MJ, Walters M, Fleet M, Anandarajah J, Sriskandan S, Mitchell JA. Cigarette smoke inhibits macrophage sensing of Gram-negative bacteria and lipopolysaccharide: relative roles of nicotine and oxidant stress. *Br J Pharmacol* 2008;153:536–543.
15. Witherden IR, Vanden Bon EJ, Goldstraw P, Ratcliffe C, Pastorino U, Tetley TD. Primary human alveolar Type II epithelial cell chemokine release: effects of cigarette smoke and neutrophil elastase. *Am J Respir Cell Mol Biol* 2004;30:500–509.
16. Pryor WA, Stone K. Oxidants in cigarette smoke: radicals, hydrogen peroxide, peroxynitrate, and peroxynitrite. *Ann N Y Acad Sci* 1993; 686:12–27.
17. Dalle-Donne I, Aldini G, Carini M, Colombo R, Rossi R, Milzani A. Protein carbonylation, cellular dysfunction, and disease progression. *J Cell Mol Med* 2006;10:389–406.
18. Dalle-Donne I, Carini M, Orioli M, Vistoli G, Regazzoni L, Colombo G, Rossi R, Milzani A, Aldini G. Protein carbonylation: 2,4-dinitrophenylhydrazine reacts with both aldehydes/ketones and sulfenic acids. *Free Radic Biol Med* 2009;46:1411–1419.
19. Stadtman ER. Oxidation of free amino acids and amino acid residues in proteins by radiolysis and by metal-catalyzed reactions. *Annu Rev Biochem* 1993;62:797–821.
20. Vlahos R, Bozinovski S, Jones JE, Powell J, Gras J, Lilja A, Hansen MJ, Gualano RC, Irving L, Anderson GP. Differential protease, innate immunity, and Nf-kappaB induction profiles during lung inflammation induced by subchronic cigarette smoke exposure in mice. *Am J Physiol Lung Cell Mol Physiol* 2006;290:L931–L945.
21. Bozinovski S, Jones J, Beavitt SJ, Cook AD, Hamilton JA, Anderson GP. Innate immune responses to LPS in mouse lung are suppressed and reversed by neutralization of GM-CSF via repression of TLR-4. *Am J Physiol Lung Cell Mol Physiol* 2004;286:L877–L885.
22. Mbawuike IN, Herscowitz HB. MH-S, a murine alveolar macrophage cell line: morphological, cytochemical, and functional characteristics. *J Leukoc Biol* 1989;46:119–127.
23. Liu K, Anderson GP, Bozinovski S. DNA vector augments inflammation in epithelial cells via EGFR-dependent regulation of TLR4 and TLR2. *Am J Respir Cell Mol Biol* 2008;39:305–311.
24. Liu K, Gualano RC, Hibbs ML, Anderson GP, Bozinovski S. Epidermal growth factor receptor signaling to Erk1/2 and STATS controls the intensity of the epithelial inflammatory responses to rhinovirus infection. *J Biol Chem* 2008;283:9977–9985.
25. Moodie FM, Marwick JA, Anderson CS, Szulakowski P, Biswas SK, Bauter MR, Kilty I, Rahman I. Oxidative stress and cigarette smoke alter chromatin remodeling but differentially regulate NF-kappaB activation and proinflammatory cytokine release in alveolar epithelial cells. *FASEB J* 2004;18:1897–1899.
26. Lang T, Mansell A. The negative regulation of Toll-like receptor and associated pathways. *Immunol Cell Biol* 2007;85:425–434.
27. Hasday JD, Bascom R, Costa JJ, Fitzgerald T, Dubin W. Bacterial endotoxin is an active component of cigarette smoke. *Chest* 1999;115:829–835.
28. Larsson L, Szponar B, Pehrson C. Tobacco smoking increases dramatically air concentrations of endotoxin. *Indoor Air* 2004;14:421–424.
29. Berenson CS, Garlipp MA, Grove LJ, Maloney J, Sethi S. Impaired phagocytosis of nontypeable *Haemophilus influenzae* by human alveolar macrophages in chronic obstructive pulmonary disease. *J Infect Dis* 2006;194:1375–1384.
30. Richens TR, Linderman DJ, Horstmann SA, Lambert C, Xiao YQ, Keith RL, Boe DM, Morimoto K, Bowler RP, Day BJ, *et al.* Cigarette smoke impairs clearance of apoptotic cells through oxidant-dependent activation of RhoA. *Am J Respir Crit Care Med* 2009;179:1011–1021.
31. Minematsu N, Blumental-Perry A, Shapiro SD. Cigarette smoke inhibits engulfment of apoptotic cells by macrophages through

inhibition of actin rearrangement. *Am J Respir Cell Mol Biol.* 2011;44:472–482.
32. Banan A, Zhang Y, Losurdo J, Keshavarzian A. Carbonylation and disassembly of the F-actin cytoskeleton in oxidant induced barrier dysfunction and its prevention by epidermal growth factor and transforming growth factor alpha in a human colonic cell line. *Gut* 2000;46:830–837.
33. Bizzozero OA, Reyes S, Ziegler J, Smerjac S. Lipid peroxidation scavengers prevent the carbonylation of cytoskeletal brain proteins induced by glutathione depletion. *Neurochem Res* 2007;32:2114–2122.
34. Smerjac SM, Bizzozero OA. Cytoskeletal protein carbonylation and degradation in experimental autoimmune encephalomyelitis. *J Neurochem* 2008;105:763–772.
35. Taylor AE, Finney-Hayward TK, Quint JK, Thomas CM, Tudhope SJ, Wedzicha JA, Barnes PJ, Donnelly LE. Defective macrophage phagocytosis of bacteria in COPD. *Eur Respir J* 2010;35:1039–1047.
36. Muller T, Gebel S. The cellular stress response induced by aqueous extracts of cigarette smoke is critically dependent on the intracellular glutathione concentration. *Carcinogenesis* 1998;19:797–801.
37. Rahman I, MacNee W. Oxidative stress and regulation of glutathione in lung inflammation. *Eur Respir J* 2000;16:534–554.
38. Dalle-Donne I, Rossi R, Colombo G, Giustarini D, Milzani A. Protein S-glutathionylation: a regulatory device from bacteria to humans. *Trends Biochem Sci* 2009;34:85–96.
39. Reynaert NL, van der Vliet A, Guala AS, McGovern T, Hristova M, Pantano C, Heintz NH, Heim J, Ho YS, Matthews DE, *et al.* Dynamic redox control of NF-kappaB through glutaredoxin-regulated S-glutathionylation of inhibitory kappaB kinase beta. *Proc Natl Acad Sci USA* 2006;103:13086–13091.
40. Marshall HE, Hess DT, Stamler JS. S-nitrosylation: physiological regulation of NF-kappaB. *Proc Natl Acad Sci USA* 2004;101:8841–8842.
41. Into T, Inomata M, Nakashima M, Shibata K, Hacker H, Matsushita K. Regulation of MYD88-dependent signaling events by S nitrosylation retards Toll-like receptor signal transduction and initiation of acute-phase immune responses. *Mol Cell Biol* 2008;28:1338–1347.
42. Park SW, Huq MD, Hu X, Wei LN. Tyrosine nitration on p65: a novel mechanism to rapidly inactivate nuclear factor-kappaB. *Mol Cell Proteomics* 2005;4:300–309.
43. Lin CC, Su TH, Wang TS. Protein carbonylation in THP-1 cells induced by cigarette smoke extract via a copper-catalyzed pathway. *Chem Res Toxicol* 2009;22:1232–1238.
44. Bernhard D, Csordas A, Henderson B, Rossmann A, Kind M, Wick G. Cigarette smoke metal–catalyzed protein oxidation leads to vascular endothelial cell contraction by depolymerization of microtubules. *FASEB J* 2005;19:1096–1107.
45. Maisonneuve E, Ducret A, Khoueiry P, Lignon S, Longhi S, Talla E, Dukan S. Rules governing selective protein carbonylation. *PLoS ONE* 2009;4:e7269.
46. Starosta V, Griese M. Protein oxidation by chronic pulmonary diseases in children. *Pediatr Pulmonol* 2006;41:67–73.
47. Mikerov AN, Umstead TM, Gan X, Huang W, Guo X, Wang G, Phelps DS, Floros J. Impact of ozone exposure on the phagocytic activity of human surfactant protein A (SP-A) and SP-A variants. *Am J Physiol Lung Cell Mol Physiol* 2008;294:L121–L130.